JNAOE
©SNAK, 2009

Inter J Nav Archit Oc Engng (2010) 2:57~67
http://dx.doi.org/10.2478/IJNAOE-2013-0020

Performance evaluation of an underwater body and pumpjet by model testing in cavitation tunnel

Ch. Suryanarayana[1], B. Satyanarayana[2], K. Ramji[3]

[1]*Naval Science and Technological Laboratory, Visakhapatnam, India*
[2]*Andhra University, Visakhapatnam, India*
[3]*Department of Mechanical Engineering, AU College of Engineering, Visakhapatnam, India*

ABSTRACT: *Experimental investigations were carried out on an Axi-symmetric Body Model fitted with Pump-jet Propulsor (PJP) in the Cavitation Tunnel at Naval Science and Technological Laboratory (NSTL). The tests were intended for evaluating the propulsion characteristics of the body and propulsor. The self propulsion point of the model for two configurations was determined after finding the corrections for tunnel blockage effects and differences in model length at zero trim. The results were found to match closely with the towing tank results. The rotor and stator torques also matched closely over full range of experiment.*
Further experiments were carried out on the body at 4.5° angle of trim to investigate the propulsive performance and assess the operational difficulties in the sea. The results indicated an increase in resistance and decrease in rotor thrust; but the balance of torques between the rotor and stator was undisturbed, causing no concern to vehicle roll.

KEY WORDS: Pump-jet; Cavitation; Cavitation tunnel; Propulsion; Experimental techniques; Hydrodynamics.

INTRODUCTION

Pump-jet concept was introduced in the field of Naval Architecture quite early as ducted propeller using a decelerating duct. It has become popular recently for high speed applications due to its enhanced cavitation performance, very low radiated noise and protection to propeller blades. It suits very well for torpedo and submarine applications. With the development of high power engines, and demand for high speeds, better cavitation performance and torque balance, the ducted propeller has transformed into pump-jet. Pumpjet is incorporated with stator vanes to straighten the slip stream swirl in order to achieve good torque balance.

Though the concept has originated from naval architecture discipline, many mechanical engineers have contributed for development of the technology. A brief account of the evolution of the pump-jet knowhow/ technology is detailed in the following paragraphs. Wislicenus and George (1960) reported that propellers have conflicting primary requirements of low machinery weight, good efficiency and good cavitation resistance. Thurston et al. (1966, 1965) reported that jet efficiency of well over 100% and propulsive efficiency approaching 100% are attainable.

Corresponding author: *Ch Suryanarayana*
e-mail: *surya_narayana_ch@yahoo.co.in*

Henderson et al. (1964) reported various issues associated with pump-jet design. They used improved cascade data but did not include the influence of cowl on the performance. Thurston and Ansler (1966) reviewed the status of marine propellers and presented their general operating regimes. Vosper and Brown (1996) reported that the submarines of United Kingdom (UK) were fitted with pump-jets. It was also reported that American Sea-wolf submarine was to be fitted with pump-jet. Mc. Cormik et al. (1956) studied the designs of contra-rotating propellers and pump-jets with reference to their efficiency and cavitation. Markatos (1984) carried out computational investigations of thick, axi-symmetric, turbulent boundary layers and wakes on bodies of revolution. Mc. Cormick et al. (1956) have published a comprehensive report on torpedo propellers including the manufacturing requirements. Turbo-machinery principles, theory and design calculations were published in a book by Wislicenus and George (1947). Das et al. (2006) carried out computational fluid dynamic analysis (CFD) simulation of PJP using finite volume formulation using k-ε model. Their predicted performance matched reasonably well with the experimental results. Stefan Ivanell (2001) carried out a detailed CFD simulation of flow over torpedo and pump-jet jointly with M/s SAAB Bofors Underwater Systems.

Suryanarayana (2003) reported on the innovative techniques employed at NSTL for manufacture of propellers using computer aided machining (CAM). Keshi et al. (2002) presented a philosophy employed for the development of

contra-rotating propellers for torpedo. Suryanarayana et al. (2006) reported the development of hydrodynamic profile and propellers for a decoy required to hover over a depth range and described the experimental technique for evaluation of performance using an instrumented decoy. They also reported about a performance evaluation technique for pump-jet through model testing in cavitation tunnel. Joubert (2004) reported the concepts essential for hydrodynamic design of a submarine. Keller (1994, 2000) published new scaling laws for predicting cavitation inception. A book was published by Horlock (1966) on axial flow turbines presenting the concepts, design, numerical analysis of gas turbines, etc. He also published another book on axial flow compressors presenting the concepts, design, and testing aspects of axial flow compressors (Harlock, 1958). Suryanarayana et al. (2010) presented an experimental technique for evaluation of pumpjet propulsor in wnd tunnel.

Naval Science and Technological Laboratory (NSTL) has initiated a program to design and develop Pump-jet propulsor of high speed under water bodies. The design of PJP was evaluated through a series of model tests in the High Speed Towing Tank (HSTT) and the Wind Tunnel (WT). In the HSTT tests, the PJP was evaluated for its propulsion characteristics. Testing in the Wind Tunnel was carried out to study the detailed pressure distribution over the cowl, the swirl in the wake, etc. Studies for the evaluation of cavitation performance and torque balance of the rotor and stator were undertaken in the Cavitation Tunnel (CT). Objective of the research work was to find a suitable technique to investigate the propulsive performance of pump-jet propulsor in Cavitation Tunnel for an axi-symmetric body using a pump-jet propulsor both with and without body trim.

The experiments in the CT are usually conducted to study the effect of cavitation on various performance parameters like resistance of the body, propeller thrust, and propeller noise under cavitation rather than their absolute values. The tunnel test section has a small cross-section and therefore significant blockage effects are expected. In the present case the blockage is about 8.3%, which is rather high. Any absolute force measurements, if necessary, have to be corrected for these tunnel wall effects. These corrections can be determined beforehand by conducting systematic experiments with the same model in the CT as well as in the HSTT. The difference in forces with and without blockage conditions can be determined experimentally for a range of speeds/conditions. These corrections can then be utilized for estimating absolute values from the CT measurements.

A similar strategy, as mentioned above, has been resorted to in analysing the propulsion data of PJP in the CT. The propulsion experiments were carried out in non-cavitating conditions to reconfirm the self propulsion point and to determine and quantify the differential torque on the rotor and stator. Cavitation inception points of different elements like rotor, stator, cowl, rudders etc., were recorded in detail. The experiment is used for predicting the performance of two submerged body configurations, Mod 1 and Mod 2 fitted with the same PJP configured to operate at the respective rpm, which have similar geometric configurations and mainly differ in the length of the parallel middle body.

The lake trials of the body indicated less than expected control surface effectiveness. The PJP was thought to be under performing, i.e., the thrust was less which consequently resulted in reduction in speed when the body was running with a trim. The data available from the trials were just for few seconds and it showed considerable change in depth. After a thorough review, it was felt that the data must be recorded at much higher sampling rate to arrive at any credible reasoning, and that it was necessary to conduct further investigations on the effect of body trim on loss of thrust and on torque balance. With this background, experiments were conducted on the body in CT at an angle of trim of 4.5º to investigate the propulsive performance and torque balance.

This paper describes the entire range of the above cavitation tunnel tests and reports the results obtained without and with a trim angle of 4.5º on the body.

BODY MODEL

The underwater body

The main particulars of the model are as given below:

Length	2917*mm*
Diameter	324*mm*
Pumpjet (Rotor) Diameter	243*mm*
Rotor Direction	Counter clock wise viewed from body aft

A set of four fins were also provided. The general arrangement of the model fitted with PJP and fins is given in Fig. 1.

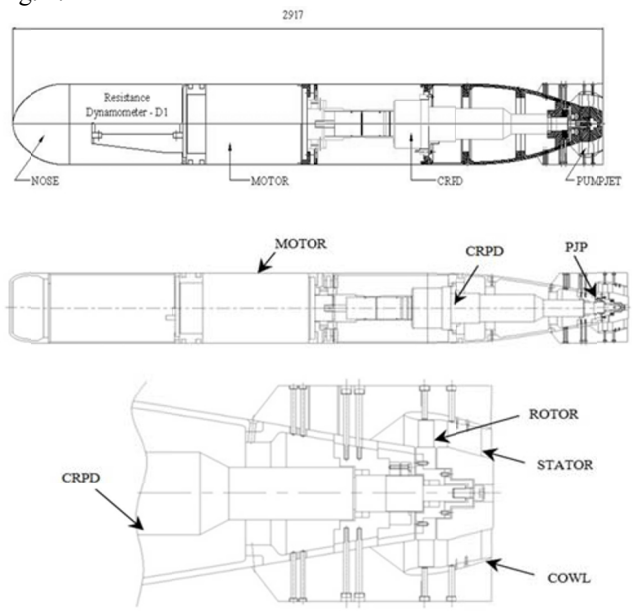

Fig. 1 Model test setup for tests in cavitation tunnel.

Pump-jet Propulsor

The Pump-jet propulsor consists of a rotating vane system (rotor) and a stationary vane system (stator) operating within an axi-symmetric diverging shroud (cowl). The stator is used to remove the swirl from the flow emanating from the rotor. The cowl retards the flow into the rotor and provides an increase in static pressure, thereby delaying cavitation. Fig. 2 shows the rotor fitted to the tail body.

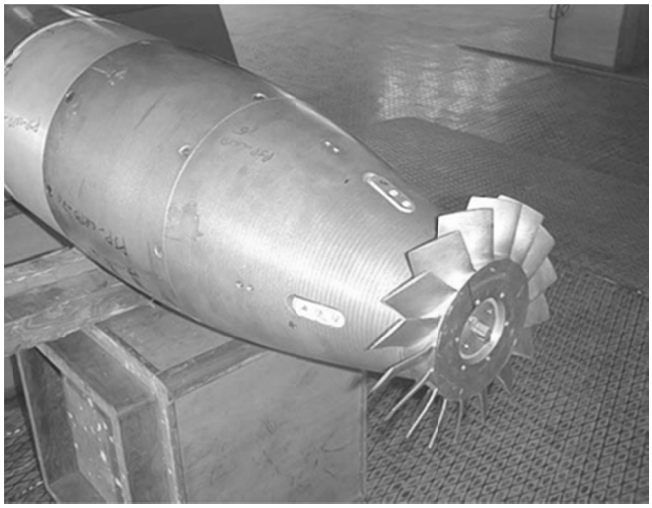

Fig. 2 Rotor with model tail body.

The stator blades are oriented in the clockwise direction when viewed from aft. Cowl is an axi-symmetric element of revolution with hydrofoil cross section surrounding both rotor and stator. For the purpose of observing cavitation in the tunnel, the cowl was manufactured from transparent Perspex material. Fig. 3 shows the rotor, stator and the transparent cowl assembled to the model tail body along with the four holding fins.

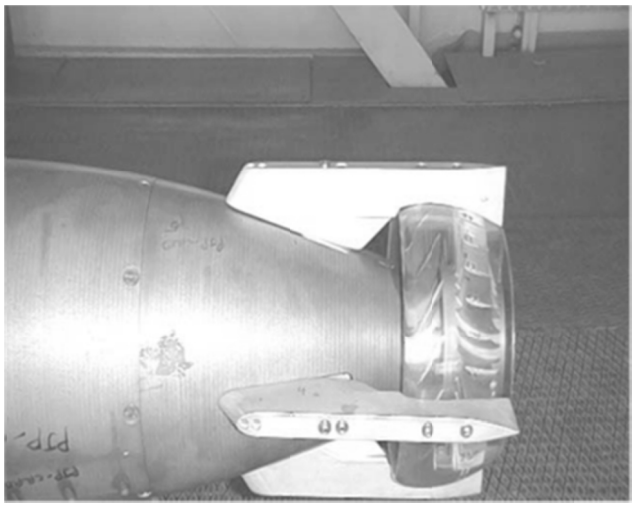

Fig. 3 PJP with model aft body.

CAVITATION TUNNEL INSTRUMENTATION

CT automatic control system (ACS)

The tunnel operation is controlled using a fully automatic control system (ACS) which regulates the set speed and pressure in the test section. The tunnel has a speed range of 0-15 *m/s* and a pressure range of 0-300 *kPa* absolute. The ACS, with the help of various pressure sensors, can achieve set speeds and pressures within accuracy of ±1 *cm/s* and ±10 *kPa*, respectively. The ACS continuously monitors the health of various systems connected to it. In case of malfunctioning of any gauge/sensor, the ACS gives visual and audible alarms. In case of an emergency, it stops and shuts down the system thereby preventing any permanent damage to it.

Data acquisition and analysis system (DAAS)

A data acquisition and analysis system (DAAS) has been designed to record various hydrodynamic test data. The motor running the propellers, and the dynamometers measuring the forces and torques on the model and propellers, are connected to the DAAS during the test. Apart from recording the data from dynamometers, the DAAS also continuously monitors the health of the dynamometers and other instrumentation connected to it. In case of any leak or overload, the DAAS gives visual and audible alarms, thereby alerting the system operators to take corrective measures.

Dynamometers

Two different types of dynamometers, namely the single component resistance dynamometer or D1, and the contra-rotating propulsion dynamometer (CRPD), were used for this experiment. The details of the dynamometers used are given below:

Single component resistance dynamometer (D1)

This dynamometer is used to measure the resistance of the model body during the resistance test, and to identify the self propulsion point during the propulsion test. The dynamometer is located at the front region of the model. The main specifications of the dynamometer are as follows:

Tow force, X1	± 3000*N*
Permissible error	± 0.7%
Max. flow speed	15*m/s*
Permissible mass of the model	250*Kg*

Contra-rotating propulsion dynamometer (CRPD)

This dynamometer is used for propulsion tests with contra-rotating propellers in both cavitating and non-cavitating regimes. There are two coaxial shafts rotating in opposite directions, connected to a single shaft motor through a contra-rotating gear. The thrust and torque on each shaft is measured by variable inductive sensing elements and the

output is recorded as an electric signal. The main specifications of the dynamometer are as follows:

Thrust on each shaft T1, T2	± 1500*N*
Torque on each shaft Q1, Q2	± 75*Nm*
Permissible error	± 0.7%
Permissible mass of either propellers	3*Kg*

CRPD is designed to operate with a pair of contra-rotating propellers. In this test the aft propeller was stationary (stator). It required careful planning to utilize the CRPD since the outer shaft was needed to be disengaged from the contra-rotating gear, but at the same time it was necessary to ensure that the forces and torques were transferred to the dynamometer sensing elements without any intermediate losses. CRPD, with its outer shaft locked, was considered ideal for simultaneous measurement of thrust and torque on both shafts. A motor along with a frequency controller was used to drive the propeller. The required rate of propeller rotation (RPS) was set from the DAAS computer, which is communicated to the frequency controller. Precise RPS ranging from –66 to +66 can be obtained with this setup.

MODEL PREPARATION IN CT

The model was held using two faired struts located longitudinally along the center line of the top surface of the test section. All the dynamometers and electric cables from the model to the connection box located on top of the test section cover were routed through these struts. Fig. 4 shows the model assembled with the PJP attached to the test section cover by two struts as mentioned above.

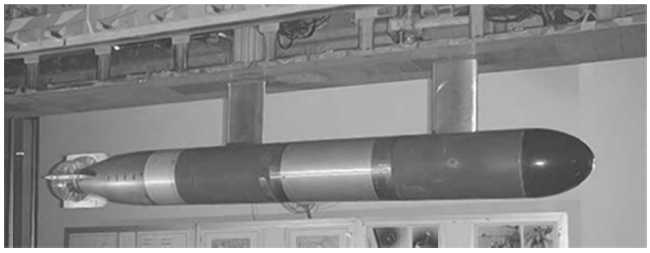

Fig. 4 Model and PJP assembly on test section.

ESTIMATION OF CORRECTIONS FROM RESISTANCE TESTS

Resistance test

The resistance of the body was measured in an earlier experiment for a 3.72*m* model corresponding to configuration Mod1. The body in this case was fitted with a faired dummy hub. The measured data is given in Table 1. A part of the parallel middle body was removed and subsequent tests were conducted with this shortened body of length 2.79 *m*. The resistance test data of the shortened body and normalized (R′) with respect to dynamic force over body cross section are given below in Table 1.

Table 1 Resistance of models of different lengths in CT.

Test Section Velocity, *V* [*m/s*]	R′			
	Measured		Estimated	
	L =3.72*m*	*L* =2.79m	*L* =2.91*m*	*L* =4.24*m*
5.00	0.205	0.186	0.188	0.215
5.50	0.203	0.189	0.191	0.211
6.00	0.201	0.186	0.188	0.210
6.50	0.200	0.184	0.186	0.209
7.00	0.198	0.184	0.186	0.205
7.50	0.196	0.185	0.186	0.203
8.00	0.195	0.183	0.185	0.202
8.50	0.195	0.183	0.185	0.202
9.00	0.195	0.183	0.185	0.201
10.00	0.194	0.183	0.185	0.200

The present series of tests with PJP were carried out with a 2.917 *m* model. This does not correspond to the scaled down length of either Mod1 (3.72 *m*) or Mod2 (4.24 *m*). In order to estimate its resistance, data from the previous resistance test of the 3.72 *m* and 2.79 *m* models were used, as nose shape and body diameter were identical. Apart from length, the shape of the tail cone was slightly different for Mod2, the effect of which is considered negligible. The resistance values are interpolated for lengths of 2.917 *m* (present model length) and 4.24 *m*. The measured and interpolated resistance values are given in Table 1 and plotted in Fig. 5.

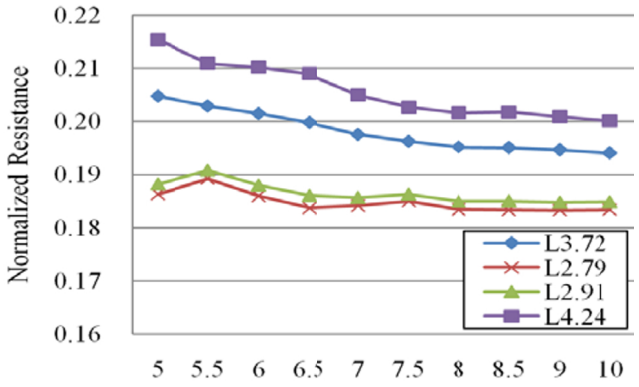

Fig. 5 Normalized resistance with different lengths in CT.

The resistance values of the parallel middle body, estimated using the international towing tank conference (ITTC) 1957 correlation (equation 1-3), were much higher than the experimentally measured values. Therefore, interpolation using the previous experimental measurements from the two lengths seems to be the best option to estimate resistance for the present model length of 2.917*m*. The incremental resistance of the parallel mid body for different

speeds were estimated using the ITTC friction correlation formulae (equation 1-3), and the results found experimentally are normalized and given in Table 2 for comparison purpose.

$$R_f = C_f \times 0.5 \times SV^2 \quad (1)$$

where R_f is the frictional resistance in N, and V is the flow velocity in m/s.

$$C_f = 0.075/(\log R_n - 2)^2 \quad (2)$$

where C_f is the coefficient of frictional resistance, and R_n is the Reynolds number.

The wetted surface area in m^2 is

$$S = 3.14 \times 0.324 \times (3.72\text{-}2.79) \quad (3)$$

Table 2 Normalized incremental resistance of parallel middle body; measured and estimated.

Test Section Velocity, V [m/s]	R' measured			R' estimated from ITTC method		
	L =3.72m	L = 2.79m	R' for L=3.72-2.79m	R_n for L=3.72m	C_f for L=3.72m	R' for L=3.72-2.79m
5	0.204735	0.186299	0.018	2.32E+07	2.60E-03	31
5.5	0.202883	0.18925	0.014	2.55E+07	2.57E-03	37
6	0.201474	0.185976	0.015	2.79E+07	2.53E-03	43
6.5	0.199803	0.183727	0.016	3.02E+07	2.50E-03	50
7	0.197527	0.184161	0.013	3.25E+07	2.47E-03	57
7.5	0.196218	0.185006	0.011	3.48E+07	2.44E-03	65
8	0.195199	0.183449	0.012	3.72E+07	2.42E-03	73
8.5	0.195069	0.183318	0.012	3.95E+07	2.39E-03	82
9	0.194661	0.183281	0.011	4.18E+07	2.37E-03	91
10	0.194062	0.183388	0.011	4.64E+07	2.34E-03	110

Estimation of blockage correction

In order to determine the correct self propulsion point of the model body, the measured values of resistance in the CT were corrected for tunnel blockage effects. Calculation of the blockage effects in the CT were made by comparing the resistance values of identical body models measured in CT and in HSTT. The Heavy Weight Body (HWB) tests in HSTT were conducted for the full scale model while the model size in the CT was scaled down to 60.62 %. Therefore, a straight forward comparison is not possible. Accordingly, an alternate method as described below was employed.

- The light weight body (LWB) models of 2.64 m length were tested in both HSTT and in CT in the same scale, the results of which are presented in Table 3. A comparison of the LWB test data shows that the resistance in HSTT (i.e., free field condition) is about 59 % of that measured in CT.
- Table 4 presents the resistance of the 3.7 m HWB model and 2.64 m LWB model, both measured in CT. The resistance of both the models is almost equal to each other at all speeds (within the dynamometer inaccuracies) even though their lengths differ by about 1.1 m. Such closeness in resistance values could be attributed to the blunt nose of LWB compared to the ogive shaped nose of the HWB. CFD analysis carried out earlier to analyse the effect of nose shape on body resistance too shows the high resistance of a flat LWB nose compared to a HWB nose. A summary of the CFD analysis is presented in Table 5 to corroborate the experimental findings.

Table 3 Normalized resistance of LWB in CT and in HSTT.

LWB with Faired Dummy Hub in CT & HSTT			
	L=2.64m	L=2.64m	Res HSTT /Res CT
	CT	HSTT	
V [m/s]	R'	R'	
6	0.205	0.121	0.59
7	0.201	0.119	0.59
7.5	0.201	0.119	0.59
8	0.199	0.117	0.59
8.5	0.198	0.117	0.59
9	0.199	0.116	0.58

Table 4 Normalized resistance of LWB & HWB in CT.

	LWB	HWB
	L=2.64m	L=3.72m
V [m/s]	R'	R'
5	0.199	0.205
6	0.205	0.201
7	0.201	0.198
7.5	0.201	0.196
8	0.199	0.195
8.5	0.198	0.195
9	0.199	0.195

CFD Analysis of Nose Shapes

In order to evaluate the effect of nose shape on resistance, CFD analysis was carried out first with LWB body fitted with 2 different nose shapes as indicated in Fig. 6. The results of CFD analysis given in Table 5 show that the drag for a flat LWB nose is 262 *Kg* for a speed . When the LWB nose is replaced by ogive HWB nose, the drag reduces to 200 Kg, i.e. a reduction of nearly 24%. This drastic reduction in drag of HWB compared to LWB due to change in nose shape, corroborates the similarities of their resistance values found experimentally.

Table 5 CFD results of body with flat and ogive nose shapes.

Profile	Length (mm)	R_n	Drag (Kg)
1: Flat LWB Nose with body	2640	4.36E+07	262
2: Ogive HWB Nose with body	2798.8	4.62E+07	200

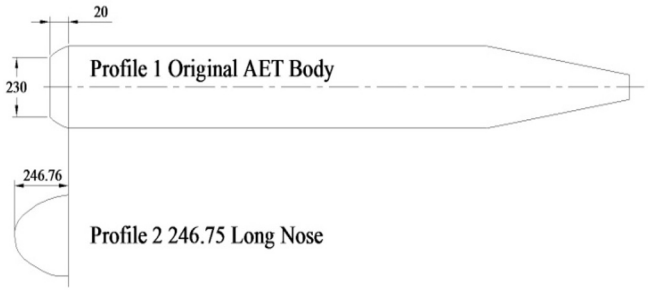

Fig. 6 Nose profiles used for CFD analysis.

Considering the above results, it is reasonable to assume that the resistance of LWB (2.64 *m*) and the HWB (3.7 *m*) in HSTT will be close to each other. Therefore, the HSTT resistance test data of LWB (already measured) can be used (as given in Table 6) for HWB (3.7*m*) since no experimental data is available for this scale. It is evident from Table 6 that the HWB resistance values in HSTT are 60% of the corresponding values in CT, which matches very well with the LWB test data in CT and HSTT (Table 3). Therefore, we have taken 60% of the HWB/Mod2 model resistance values measured in CT to get the corresponding free field values. Table 5 gives the resistance correction to be added to the CT measurements for 2.91 *m* model at different speeds to get their corresponding free field values.

Table 6 Normalized resistance data of HWB (in HSTT & CT).

HWB	CT	HSTT	Res HSTT /Res CT
	L =3.72m	L=3.72m	
V [m/s]	R'	R'	
5	0.205	0.124	0.61
6	0.201	0.121	0.6
7	0.198	0.119	0.6
8	0.195	0.117	0.6
9	0.195	0.116	0.6
10	0.194	0.115	0.59

Table 7 Normalized blockage corrections for 2.91m model.

	Res CT	Res HSTT = 0.59Res CT	BLOCKAGE CORRECTION
V (m/s)			CORR [N]
6	0.188	0.111	-114
7	0.186	0.110	-154
8	0.185	0.109	-200
9	0.185	0.109	-253
10	0.185	0.109	-312

Resistance increment due to increase in length

In order to use the data derived using the 2.91 m model instead of 3.7 *m* (Mod1) and 4.24 *m* (Mod2), suitable correction has to be determined for the increased length. Table 1 gives normalized model resistance in CT for different model lengths. Table 8 gives the correction in resistance in CT for estimating the performance of 3.7 *m* Mod2 model with data from 2.91 *m* model. Table 9 gives the correction in resistance in CT for estimating the performance of 4.24 *m* (Mod2) model with data from 2.91 *m* model.

Table 8 Resistance.

Length Correction (3.7*m*~2.91*m*)	
V (m/s)	Corr [*N*]
6	20
7	24
8	27
9	33
10	38

Table 9 Resistance Corrections.

Length Correction	
(4.24*m*~2.91*m*)	
V (m/s)	Corr [*N*]
6	33
7	39
8	44
9	54
10	63

PROPULSION TEST

Test procedure

The outer shaft of the CRPD was connected to the stator fixed to the cowl supported on four fins and the inner shaft was connected to the rotor. Each cycle of test was carried out at a constant tunnel flow speed. The advance ratio *J* is adjusted by varying the propeller RPS. In this series of tests, it was felt prudent to apply a positive static pressure of 50 *kPa* (w.r.t. atmosphere) in the test section so that the likelihood of cavitation on any appendages or other elements was avoided even at the highest flow speeds. The tests were conducted for flow speeds of 6, 7, 8, 9 and 10 *m/s* and *J* from 2.45 to 1.85 as the design *J* value is 2.18 for Mod1 and 1.91 for Mod2.

Propulsion test data

The propulsion test data at tunnel speed of 9 *m/s* is given in Fig 7a and 7b.

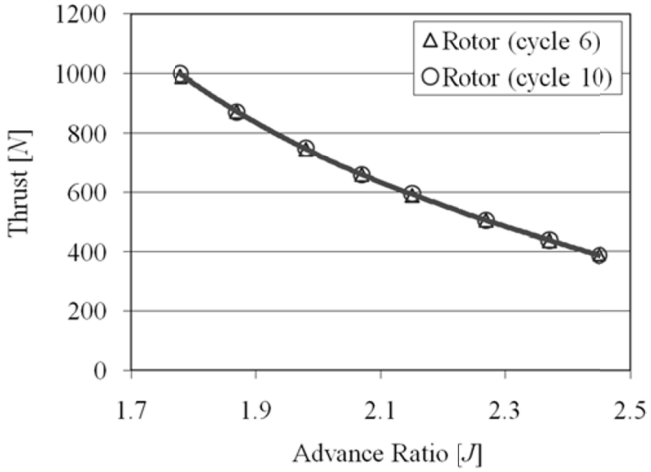

Fig. 7a Rotor thrusts at tunnel speed of 9 *m/s*.

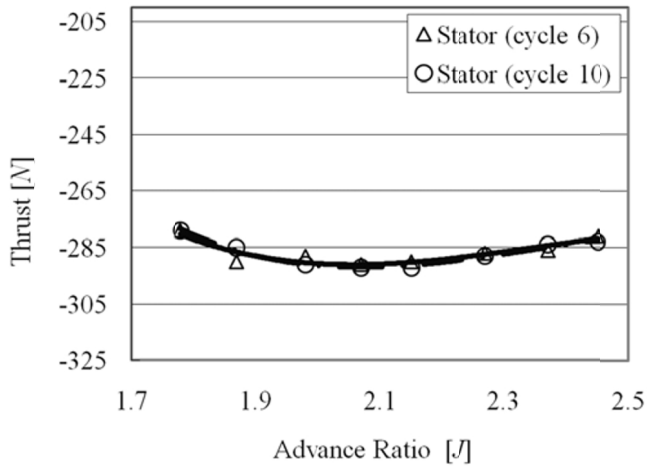

Fig. 7b Stator thrusts at tunnel speed of 9 *m/s*.

Discussions

The following inferences can be directly made from the measured data. The force on the stator, cowl and fin combination is a drag force (as indicated by the negative sign at Fig. 7), which remains almost constant with advance ratio (*J*) at a given speed. The rotor thrust increases as expected with increase in RPS. The two cycles superimposed in Fig. 7 (cycle 6 and 10) show excellent repeatability of the measurements. The stator and rotor torques balance closely with each other for full range of measurements (Fig. 8). As RPS increases and *J* reduces, the rotor thrust increases and the net force on D1 (Net Force = Resistance – Thrust) decreases. A sufficiently high *J* at which the net force

becomes zero is considered the self-propulsion point of the model included with the blockage resistance.

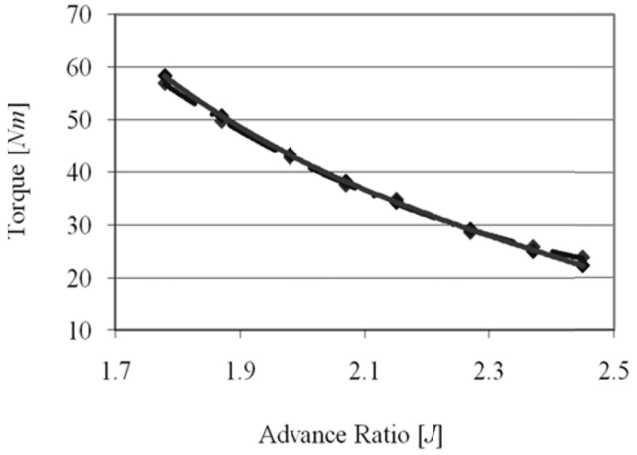

Fig. 8 Rotor and Stator torques at tunnel speed of 9 *m/s*.

Determination of the self-propulsion point

Unlike in HSTT, the tests in CT are affected by blockage and this effect is considered and corrected to arrive at a reasonably accurate self propulsion point. In this case, the change in length of model is also accounted for determining the self propulsion point. As no test was done with the dummy hub of PJP, the conventional way of calculating a Reynolds number correction by using the bare body resistance and appended resistance for correctly estimating the self- propulsion point, was not feasible in the present case. There is an uncertainty in the hull propeller interaction effects also. Therefore, the propulsion data was analyzed in a slightly different way. The force measured by Single component resistance dynamometer (D1) is the net resultant of all resistance forces and thrust forces. Self-propulsion point is the instant when this net force is zero, or the net resistance equals to net thrust. By correcting the measured D1 force for blockage effects and length change, one can get the self propulsion point in the free field condition. Therefore, the net forces measured by D1 are corrected with the applicable speed dependent corrections determined earlier. The second correction to be applied is that due to change in length. In this case, the model length was increased from 2.91 *m* to 3.7 *m* in the case of Mod1 body. Similarly, correction in net force (measured by D1) was made for Mod2 body length of 4.24 *m* also. The data measured by D1 is plotted against *J* as indicated by the curve model-body-in CT in Fig 9. The resistance decreases after incorporating the blockage correction and the corresponding data is plotted as "Resistance with Blockage Correction". Further, the data is corrected for Mod1 length and is plotted as "Resistance with Blockage and Length Correction–Mod1". The self-propulsion takes place at J = 1.955. The data corresponding to Mod2 length is plotted as "Resistance with Blockage and Length Correction – Mod2". The self- propulsion in this case is at J = 1.925.

The above calculations were repeated for other test speeds of 6, 7, 8 and 10 *m/s*. The self-propulsion point was determined for each speed and the resulting data are plotted in Fig. 10.

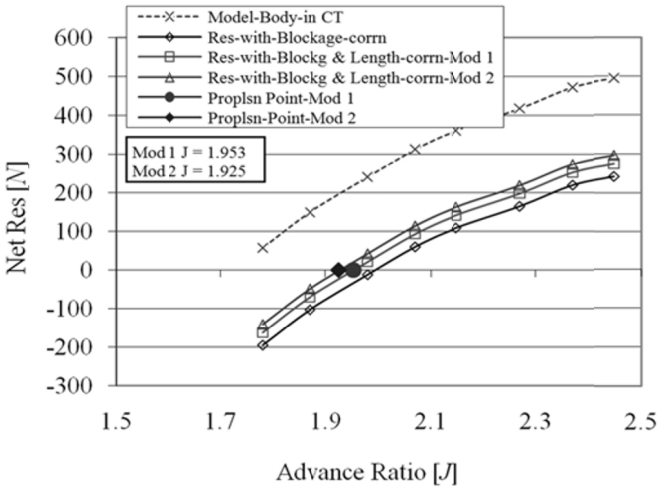

Fig. 9 Propulsion characteristics of PJP for Mod 1 and Mod 2.

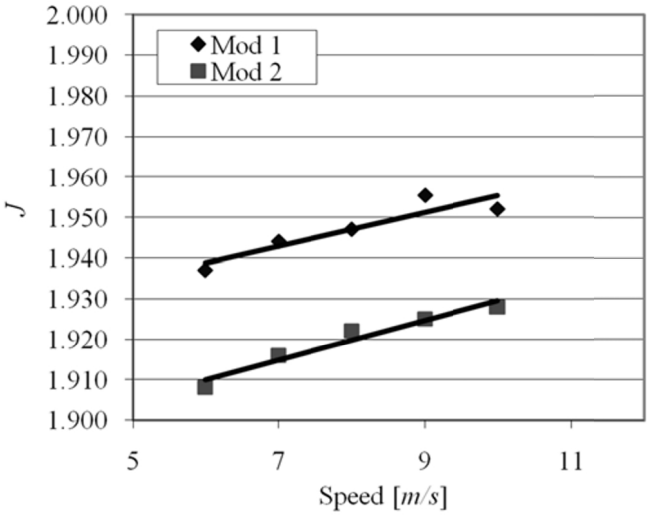

Fig. 10 Self propulsion *J* at different speed.

If there were no scale effects at all the testing speeds, the self-propulsion J would have been identical. However, our results in Fig 10 show a gradual increase in J with speed. This is because of the increase in Reynolds number with increase in speed, which results in a consequent decrease in the frictional resistance coefficient (C_f). The reduction in C_f from model to full scale reduces the total resistance by about 10% in Mod1 and about 8% in Mod2. Therefore, the self-propulsion J would increase by a similar magnitude when extrapolated from model to full scale. This would result in a self-propulsion J = 2.147 for Mod1 and J = 2.08 for Mod2.

Comparison with HSTT results

Mod 1

The tests in HSTT indicate that self-propulsion in the model takes place at J = 1.986. As the test Reynolds number

is much lower than the prototype value, the drag coefficient is expected to decrease at prototype Reynolds number by at least 10% and result in self propulsion at J = 2.18. CT results for the model indicate a self-propulsion point at J = 1.952. At the full scale Reynolds number, the resistance coefficient would come down and self-propulsion would be at J = 2.147

Mod 2

The tests in HSTT with Mod 2 body with PJP indicate that the self propulsion takes place at J =1.984 The CT test indicates a model self-propulsion at J = 1.928. The full scale propulsion is estimated to be at J = 2.08

PROPULSION TEST WITH AN ANGLE OF TRIM

Requirement

The lake trials of the body indicated less than expected control surface effectiveness. The PJP was thought to be under performing, i.e., the thrust was less which consequently resulted in reduction in speed when the body was at an angle of attack. The data available from the trials were for a few seconds and showed drastic changes in depth. After a thorough review, it was felt essential to investigate the effect of body trim on possible loss of thrust, torque balance and increase in resistance. In order to have an estimate of the effect of angle of attack or trim on the rotor thrust, propulsion tests were carried out with the body model with an angle of attack of 4.5° to the direction of flow. The test and results are described below.

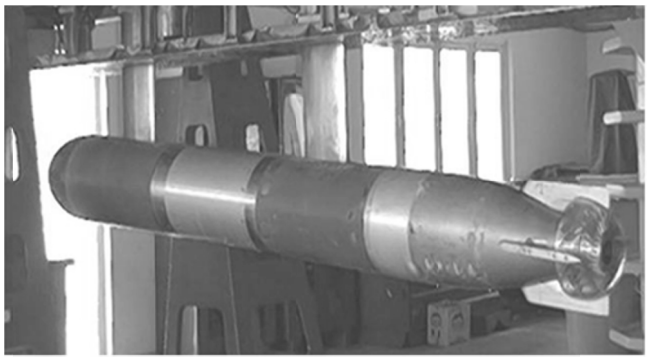

Fig. 11 Model at angle of attack of 4.5°.

Test setup

The torpedo model used in the earlier propulsion tests was inclined in the longitudinal vertical plane at an angle of attack of 4.5°, by raising the forward strut. The model after inclination is shown in Fig. 11.

Test procedure

The test procedure followed was identical to that for the propulsion tests carried out at 0° angle of attack. All the tests were conducted at positive static pressure of 50 *kPa* in the test section. The advance coefficient J was varied at a constant tunnel flow speed by varying the rotor RPS. At each value of J, the rotor thrust, torque, RPS, stator torque and the net force on the D1 dynamometer were measured. It was not possible to measure the drag/thrust force on the stator cowl combination in this test. As the main objective of the test was to find the drop in thrust produced by the rotor, this drawback was not considered very serious.

Test results

The test data at a tunnel speed of 10 *m/s* for 0° and 4.5° angle of attack are given Table 10 and Table 11, respectively.

Table 10 Propulsion data at V=10*m/s* and angle of trim=0°.

Angle of Attack 0°				
Advance Coefficient	Rotor	Rotor	Stator	D1
J	Thrust[N]	Torque [Nm]	Torque	Res [N]
2.46	461	26.5	23.9	611
2.36	533	30.8	24.8	567
2.26	614	35.7	30	509
2.17	692	40.3	35.2	455
2.07	797	46.3	42.8	383
1.97	918	53.7	50.1	285

Table 11 Propulsion data at V=10*m/s* and angle of trim=4.5°.

Angle of Attack 4.5°				
Advance Coefficient	Rotor	Rotor	Stator	D1
J	Thrust [N]	Torque [Nm]	Torque [Nm]	Res [N]
2.46	431	26.2	25.5	701
2.36	499	30.2	30.9	651
2.25	584	35.4	37.2	594
2.18	657	39.7	39.2	551
2.07	767	46.4	46.4	466
1.97	886	53.8	52.5	380
1.89	1000	60.9	63.7	284
1.78	1160	70	70.4	162

The net increase in resistance and the net reduction in thrust with change in the angle of attack from 0° to 4.5° at each value of J are given in the Table 12.

Table 12 Change of resistance and thrust with trim, V=10 *m/s*.

Advance Coefficient J	Δ Res [N]	Δ Thrust [N]
2.46	90	-30
2.36	84	-34
2.26	85	-30
2.17	96	-35
2.07	83	-30
1.97	95	-32

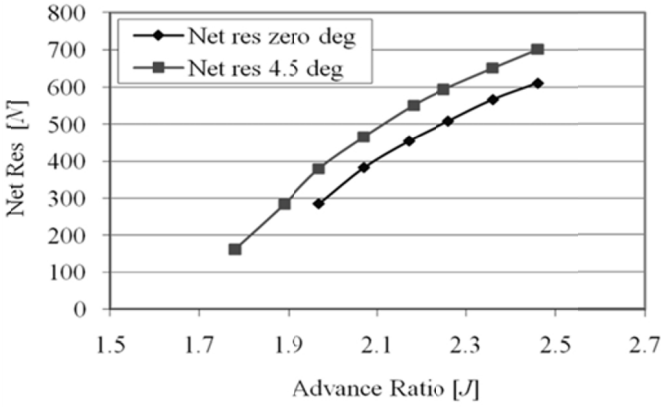

Fig. 12 Resistance of body at 0° and 4.5° trim.

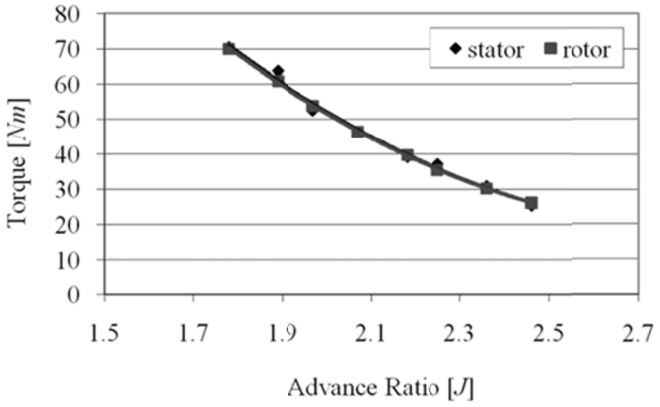

Fig. 13 Torque balance at 10*m/s* and trim of 4.5°.

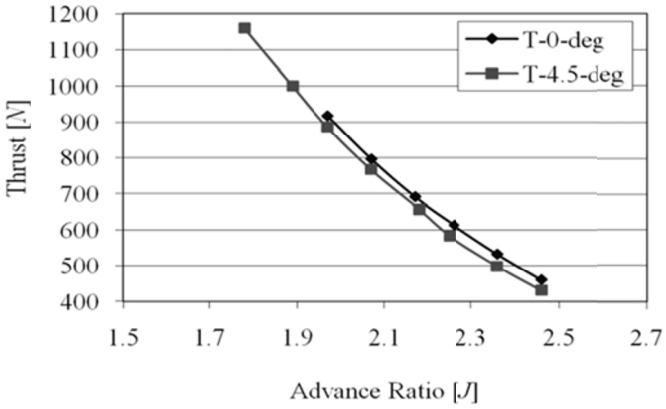

Fig. 14 Rotor thrust at 10*m/s* and trim of 0° and 4.5°.

Discussion on propulsion tests with trim angle

Increase in resistance

The measured change in net resistance with increase in angle of attack from 0° to 4.5° showed almost a constant increase of 90 N for all values of J. The change in the rotor thrust is negative, indicating a reduction in the thrust generated as the vehicle takes an angle of attack. The reduction in thrust is also almost constant and ranged between 30-35 N over the entire range of advance coefficient. Therefore, it can be concluded that effectively the resistance of the body is increased by about 60 N at 10 *m/s* speed at the angle of attack of 4.5°.

Decrease in rotor thrust

The reduction in rotor thrust may be probably due to insufficient inflow into the rotor as it is enclosed by the cowl. The reduction is about 5% at this angle of attack.

Torque balance

The results shown in Fig 13 indicate that the torque balance between rotor and stator is maintained quite well even at 4.5° angle of attack.

CONCLUSIONS

- The self-propulsion points for Mod 1 in full scale and in HSTT were found to be at advance coefficient of 2.147 and 2.18, respectively. The corresponding self-propulsion points for Mod 2 were at advance coefficient of 2.08 and 1.984 for full scale and for HSTT, respectively. The results are reasonably accurate for any such applications.

- The propulsion experiments have confirmed that there is a very close torque balance between the rotor and stator of the PJP at zero trim.

- The torque balance between the stator and the rotor could be attained even with the body trim thereby eliminating the apprehensions of body roll and its affects.

- Reduction in rotor thrust for the design could be estimated reasonably well using the technique.

- The CT results were found reasonably close to the HSTT results. It suggests that systematic resistance and propulsion tests of submerged models can be done entirely in the CT without the apprehensions of tunnel wall effects.

ACKNOWLEDGEMENT

This work was undertaken with the support and funding from Defense Research and Development Organization, Ministry of Defense, India. The authors express their sincere gratitude to Govt. of India, Dr. V Bhujanga Rao, Director and Shri PK Panigrahi, Additional Director of NSTL for permitting to publish the work. The authors wish to thank officers and staffs of HRW, NSTL for contributions made in CFD, model manufacture and testing activities. The authors also thank Shri M Nageswara Rao and Shri H Keshi for their valuable support in accomplishing the task and in preparing the manuscript of the paper. Authors express their sincere gratitude to Cmde N Banerjee for the encouragement and support given throughout this work.

REFERENCES

Wislicenus, G. F., 1960. Hydrodynamics and propulsion of submerge bodies. *J. Am. Rocket Soc.* 30(12), pp. 1140-1148.

Thurston, S. and Ansler, R.C., 1966. Review of marine propellers and ducted propeller propulsive devices. *J. Aircraft*, 3(3). pp. 255-261.

Thunston, S. and Evanbar, M.S., 1965. Efficiency of propulsor on body of revolution including boundary layer fluid. *Journal of Aircraft*, 3, pp. 270-277.

Henderson R.E. McMahon J.F. and Wislicenus G.F., 1964. A method for design of pumpjets. *ORL Report* No. 63-0209-0-7, Pennsylvania State University, 15 May 1964.

Vosper P.L. and Brown A.J., 1996. Pumpjet propulsion - a British splendid achievement. *J. Naval Engineering*, 36(2),

McCormick, B.W. Eisenhuth, J.J. and Lynn, J.E., 1956. *A Study of torpedo propellers*–Part I. Ordnance Research Laboratory, Pennsylvania State University, Report NOrd. 16597-5.

Markatos, N.C., 1984. The Computation of thick axi-symmetric boundary layers and wakes around bodies of revolution. *Proceedings of Institution of Mechanical Engineers*, 198(4), pp. 51-62.

McCormick, B.W. and Eisenhuth, J.J., 1956. *A Study of torpedo propellers*–Part II. Ordnance Research Laboratory, Pennsylvania State University, Report NOrd. 16597-13.

Wislicenus, G.F., 1965. *Fluid mechanics of turbo-machinery*. Volume I and II, Dover Publication, New York, USA.

Das, H.N. Jayakumar, P. and Saji, V.F., 2006. CFD examination of interaction of flow on high-speed submerged body with pumpjet propulsor. *5th Int. Conference on High Performance Marine Vehicles*, Australia , 8-10 November 2006.

Stefan Ivanell, 2001. *Hydrodynamic simulation of a torpedo with pumpjet propulsion system*. Master thesis, Royal Institute of Technology, Stockholm, Sweden

Suryanarayana, Ch., 2003. Innovative CAM techniques for propeller manufacture. *3rd International Conference on Navy and Ship Building Nowadays (NSN2003)*, St Petursburg, Russia, 26-28 June 2003.

Keshi, H. Maharana, S.N. and Suryanarayana, Ch., 2002. Design philosophy of contrarotating propellers. *International Conference on Ship and Ocean Technology*, SHOT-2002, IIT, Kharagpur, India, December 2002.

Suryanarayana, Ch. Reddy, K.P. Mathi, S. Swamy, P.V., and Suresh R.V., 2006. Hydrodynamic design of propulsor, profile and hovering system for an expendable decoy. *International Conference in Marine Hydrodynamics 2006*, NSTL, Visakhapatnam, India

Suryanarayana, Ch. Roy, S.P. and Sateesh Kumar, M., 2006. Hydrodynamic performance evaluation of an underwater body by model testing in cavitation tunnel. *International Conference in Marine Hydrodynamics* 2006, NSTL, Visakhapatnam, India.

Joubert P.N., 2004. *Some aspects of submarine design, part:1 – Hydrodynamics*. Report No. DSTO-TR-1622, Department of defense, Australian Government, Oct 2004.

Keller, A.P., 1994. New scaling laws for hydrodynamic cavitation inception. *The 2nd International Symposium on Cavitation*, Tokyo, Japan.

Keller, A.P., 2000. Cavitation scale effects- A representative of its visual appearance and empirically found relations. In : *NCT'50 International Conference of Propeller Cavitation*, Newcastle Upon Tyne, UK.

Harlock, J.H., 1966. *Axial flow turbines - fluid mechanics and thermodynamics*. Butterworth Publishers, London.

Harlock, J.H., 1958. *Axial flow compressors - fluid mechanics and thermodynamics*. Butterworth Publishers, London.

Suryanarayana, Ch., Satyanarayana, B., Ramji, K. and Saiju, A., 2010. Experimental evaluation of pumpjet propulsor for an axisymmetric body in wind tunnel. *Inter J Nav Archit Oc Engng,*2(1), pp.24-33.